Index

(a)

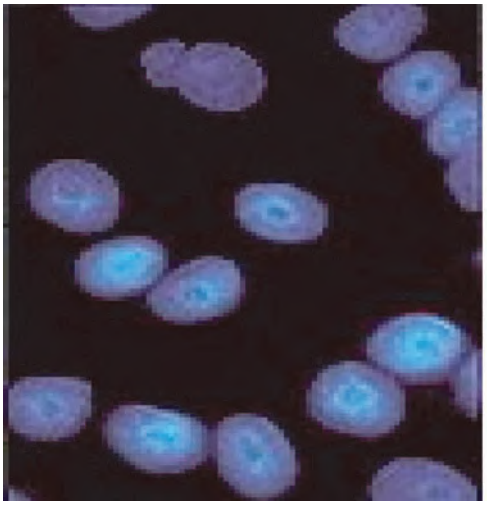

(b)

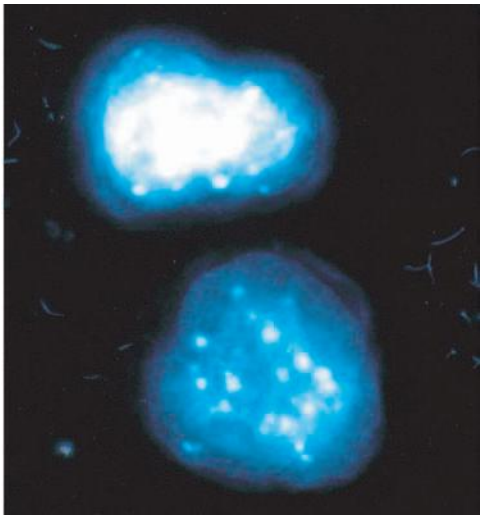

Fig. 2.4. Staining for mycoplasma in cells. (a) A Hoechst negative stain, with the dye staining cellular DNA in the nucleus and thus showing nuclear fluorescence. (b) A Hoechst positive stain, showing staining of mycoplasma DNA in the cytoplam of the cells.

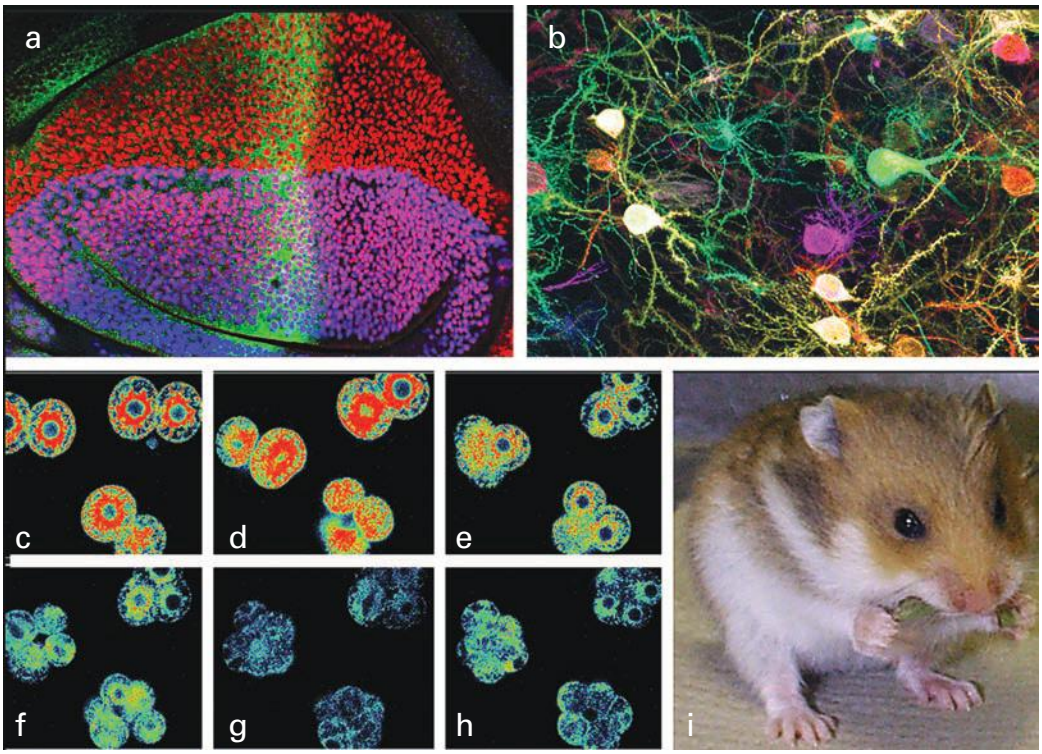

Fig. 4.13. Optical sectioning. Optical sections produced using LSCM (a and b) and multiple photon imaging (c). (a) Triple labelled *Drosophila* third instar wing imaginal disc. The images were produced using an air-cooled 25 mW krypton argon laser, which has three major lines at 488 nm (blue), 568 nm (yellow) and 647 nm (red). The three fluorochromes used were fluorescein (excitation 496 nm; emission 518 nm), lissamine rhodamine (excitation 572 nm; emission 590 nm) and cyanine 5 (excitation 649 nm; emission 666 nm). The images were collected simultaneously as single optical sections into the red, the green and the blue channels, respectively, and merged as a three-colour (red/green/blue) image (see Fig. 4.11). The image shows the expression of three wing-patterning genes; *vestigial* (in red), *apterous* (in blue) and *CiD* (in green). Regions of overlap of gene expression appear as an additive colour in the image. (b) Multicolour neurones labelled with combinations of lipophilic dyes. (c) Two photon images of three living hamster embryos labelled with the mitochondrial dye Mitotracker X rhodamine. The three embryos were imaged over a 24 h period. Images (c) to (h) are representative images collected from the time-lapse series. One of the three embryos was transferred to an adult female, who later produced 'Laser' – a living testament to the viability of multiple photon imaging. (Images kindly provided by (a) Jim Williams and Sean Carroll, (b) Wenbio Gan and Jeff Lichtman, and (c) Jayne Squirrell and Barry Bavister.)

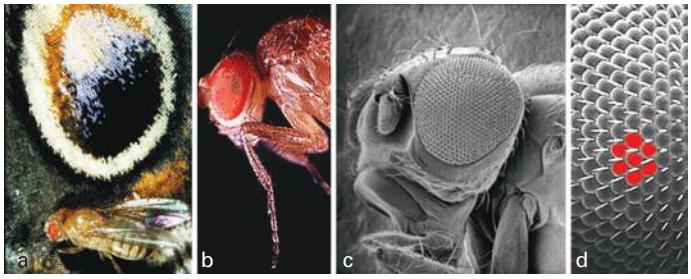

Fig. 4.17. Image surfaces using the light microscope (stereomicroscope) and in the electron microscope (scanning electron microscope). Images produced using the stereomicroscope (a) and (b) and the scanning electron microscope (c) and (d). A stereomicroscope view of a fly (*Drosophila melanogaster*) on a butterfly wing (*Precis coenia*). (a) Zoomed in to view the head region of the red-eyed fly (b). SEM image of a similar region of the fly's head (c) and zoomed more to view the individual ommatidia of the eye (d). Note that the stereomicroscope images can be viewed in real colour whereas those produced using the SEM are in greyscale. Colour can be added to EM images only digitally (d). (Images (b), (c) and (d) kindly provided by Georg Halder.)

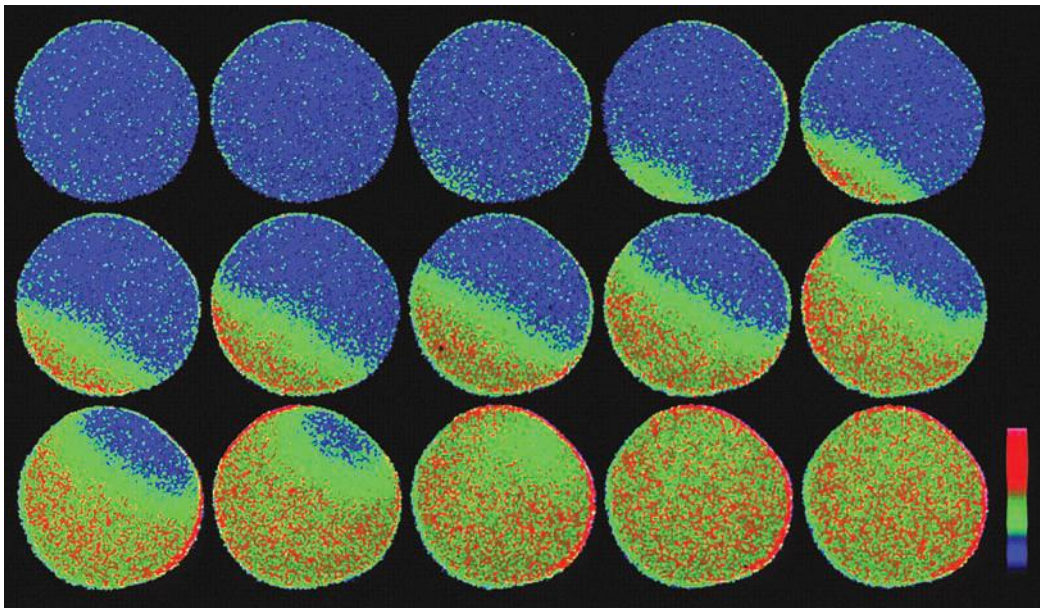

Fig. 4.21. Calcium imaging in living cells. A fertilisation-induced calcium wave in the egg of the starfish. The egg was microinjected with the calcium-sensitive fluorescent dye fluo-3 and subsequently fertilised by the addition of sperm during observation using time-lapse confocal microscopy with a 40× water immersion lens. An optical section located near the egg equator was collected every 4 s using the normal scan mode accumulated for two frames, and afterwards the images were corrected for offset and ratioed by linearly dividing the initial pre-fertilisation image into each successive frame of the time-lapse run. The ratioed images were then prepared as a montage and outputted with a pseudocolour look-up table: blue regions represent low ratios, and free calcium levels; green regions depict intermediary levels; and red areas depict high ratios and free calcium levels. Note that the wave sweeps through the entire ooplasm. (Image kindly provided by Steve Stricker).

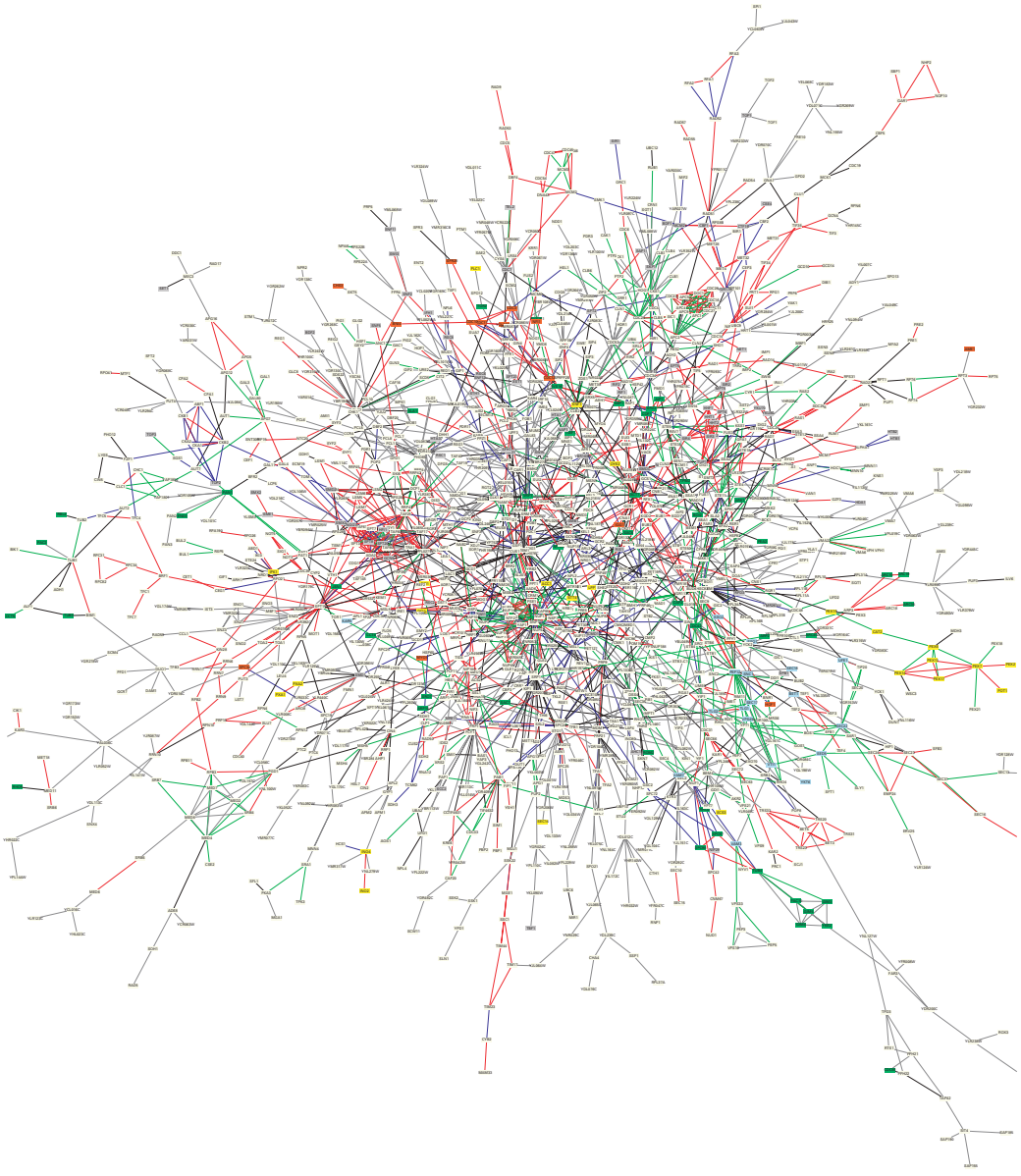

Fig. 8.11. An interaction map of the yeast proteome, assembled from published interactions (see text for details). (Courtesy of Benno Schwikowski, Peter Uetz and Stanley Fields. Reprinted with the permission of Nature Publishing Group.)

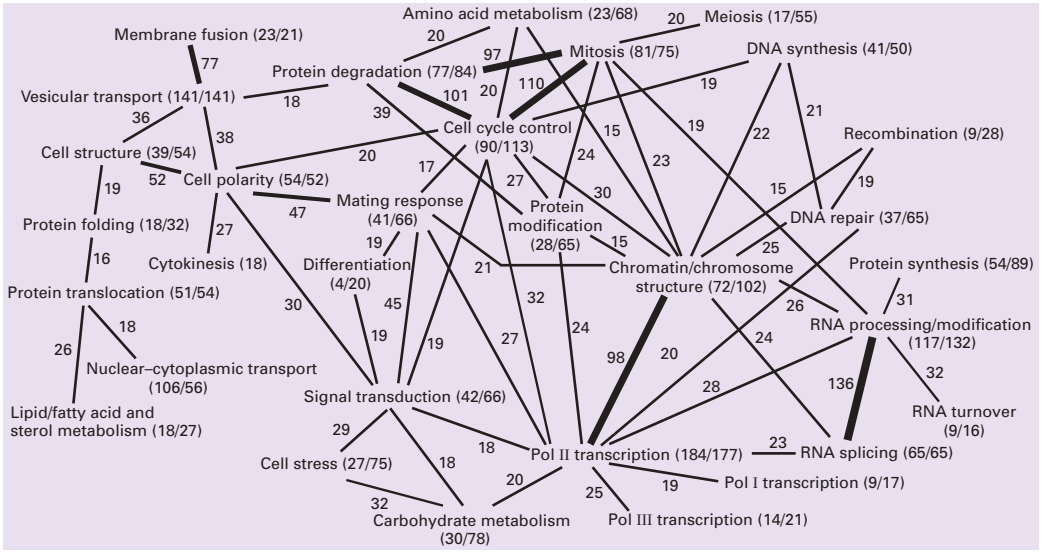

Fig. 8.12. A simplification of Fig. 8.11 identifying interactions between functional groups of proteins (see text for details). (Courtesy of Benno Schwikowski, Peter Uetz and Stanley Fields. Reprinted with the permission of Nature Publishing Group.)